Functional network dynamics in progressive multiple sclerosis

Giulia Bommarito[1,2,3], Anjali Tarun [1,2], Younes Farouj [1,2], Maria Giulia Preti[1,2], Maria Petracca[4], Amgad Droby[4], Mohamed Mounir El Mendili[4], Matilde Inglese[3,4,5], Dimitri Van De Ville[1,2]

[1]Institute of Bioengineering, Center for Neuroprosthetics, Ecole Polytechnique Fédérale de Lausanne, Geneva, Geneva 1202, Switzerland.
[2]Department of Radiology and Medical Informatics, Faculty of Medicine, University of Geneva, Geneva, Geneva 1206, Switzerland.
[3]Department of Neuroscience, Rehabilitation, Ophthalmology, Genetics, Maternal and Child Health (DINOGMI), University of Genoa, Genoa, Italy.
[4]Department of Neurology, Icahn School of Medicine at Mount Sinai, New York, NY, USA
[5]Ospedale Policlinico San Martino, IRCCS, Largo Daneo 3, 16100, Genoa, Italy.

Running title: functional dynamics in progressive MS

Keywords: progressive multiple sclerosis; resting-state functional MRI; innovation-driven co-activation patterns; default mode network; clinical disability.

Abbreviations: PMS= progressive multiple sclerosis; PP= primary progressive; SP= secondary progressive; fMRI= functional MRI; rs-fMRI: resting state functional MRI; DMN = default mode network; rs-FC: resting state functional connectivity; iCAP= innovation driven co-activation pattern; BOLD= blood-oxygenated-level dependent; FU= follow-up; HC= healthy control; EDSS= expanded disability status scale; T25FW= timed 25-foot walking; 9HPT=9-hole peg test; SDMT= symbol digit modalities test; CVLT-II= California verbal learning test second edition; BVMT-R = brief visuospatial memory test revised; WM=white matter; CSF= cerebrospinal fluid; $FD_{Power=}$ framewise displacement according to Power et al.; TA= total activation; MNI= Montreal Neurological Institute; ANCOVA = analysis of covariance; FDR = false discovery rate; PLSC = partial least squares correlation; Hipp: hippocampus; Amy: amygdala; BG: basal ganglia; Aud:

auditory; SM: sensory-motor; ECN: executive control network; AntDMN: anterior default mode network; AntIns: anterior insula; SAL: salience; TempPar: temporo-parietal; LAN: language; SecVis: secondary visual; PostDMN: posterior default mode network; TempPole: temporal pole; OFC: orbito-frontal cortex.

Abstract

Functional reorganization at the progressive stage of multiple sclerosis has received limited attention, despite the fact that functional changes are known to occur. Characterizing large-scale network dynamics at rest has the potential to provide new insights into the complexity of such functional alterations. In this case-control study, we explored the dynamic properties of large-scale functional networks during rest in 25 healthy controls and 32 patients with progressive multiple sclerosis, using the innovation-driven co-activation patterns. Thirty-five subjects also underwent a one-year follow-up examination. Partial least squares correlation analysis was applied to explore the relationship between functional dynamics and clinical disability. We observed a reduced dynamic engagement of the anterior default mode network and its coupling with the executive-control network in patients with progressive multiple sclerosis compared to controls, at baseline and follow-up. The global and motor disabilities were related to functional dynamics of subcortical, sensory-motor and posterior default mode network, while the cognitive disability was associated to the altered dynamics of anterior default mode, visual and temporal networks. These findings reveal that the anterior default mode functional recruitment and its interaction with other networks play a major role in the functional reorganization occurring during the progressive stage of multiple sclerosis. Also, the dynamic properties of large-scale functional networks are steady over one year and unveil the intricate relationship between brain function and clinical disability.

Introduction

Progressive multiple sclerosis (PMS) is characterized by neurodegeneration as prominent pathological feature and by a gradual worsening in clinical disability, occurring from the onset of the disease in the case of the primary progressive (PP) form, or after a phase characterized by relapses in the case of the secondary progressive (SP) multiple sclerosis (MS). Despite the two forms, PP and SP MS, can differ in terms of epidemiological, clinical, radiological features, and therapeutic approaches, their pathophysiological pattern is recognized as similar (Lassmann, 2019) and the two phenotypes are considered different aspects of a unique spectrum (Confavreux and Vukusic, 2006).

Functional magnetic resonance imaging (fMRI) has been widely used in the last two decades to investigate the functional changes in blood-oxygenation-level dependent (BOLD) responses occurring at various stages of MS disease. Resting state fMRI (rs-fMRI) has the advantage of being independent from the ability of a patient to understand and execute instructions to perform a specific task, and, therefore, is suited for exploring brain plasticity occurring in patients with advanced disability (Guerra-Carrillo *et al.*, 2014; Lv *et al.*, 2018). However, there are only few studies that specifically investigated resting state functional activity or connectivity (rs-FC) in patients with PMS, disclosing the presence of abnormalities involving the default mode network (DMN), the executive control and the attentional networks, related to cognitive impairment (Rocca *et al.*, 2010; Petracca *et al.*, 2017). Overall, conventional rs-FC has not been related to motor or global disability in the late stages of the disease.

Beside conventional rs-FC analysis, new dynamic approaches have recently emerged to explore the time-varying nature of FC (Preti *et al.*, 2017). Using the sliding-window methodology, the dynamics of rs-FC have been investigated in patients with clinically isolated syndrome or with relapsing-remitting MS, emphasizing the complex functional changes occurring in this disorder, in particular in relationship to the cognitive status, and showing the validity of the complementary

information a dynamic approach could offer to understand such changes (Leonardi *et al.*, 2013; Lin *et al.*, 2018; van Geest *et al.*, 2018; Cordani *et al.*, 2019; d'Ambrosio *et al.*, 2019; Eijlers *et al.*, 2019; Rocca *et al.*, 2019). However, sliding-window analysis comes with several limitations, such as the inconsistencies in the choice of the window lengths, which makes results from different studies less comparable (Preti *et al.*, 2017). So far, most of the prevailing dynamic FC approaches have also assumed a temporally segregated nature of the outcoming functional networks. Alternatively, innovation driven co-activation patterns (iCAPs) is a technique that allows to derive whole brain patterns showing regions that co-activate or co-deactivate at the same time, based on the *transients* or changes in fMRI time courses (Karahanoglu and Van De Ville, 2015). An abnormal dynamic of these brain "states" or networks and their altered co-occurrences ("coupling") have already been reported as a key measure of the pathophysiological process occurring in neurological and neuropsychiatric disorders, as well as of the functional reorganization related to therapeutic procedures (Zhuang *et al.*, 2018; Zöller *et al.*, 2019; Tuleasca *et al.*, 2020). Concurrently enabling to capture the time-varying activity of large-scale brain networks, and to unravel the interaction between different sub-components of the DMN and other networks, iCAPs seem suited to extricate functional dynamics in a heterogeneous and complex disorder such as MS, where DMN dysfunction has been described all through the disease course (Basile *et al.*, 2014; Rocca *et al.*, 2018).

Nonetheless, the dynamics of functional networks in patients in the progressive stage of the disease remains unexplored, compared to the other clinic-radiological phenotypes. Despite this, the burden of disability associated to this disease phase, the relative lack of disease modifying drugs and the potential efficacy of rehabilitation strategies, summon for a more exhaustive picture of the functional changes characterizing PMS, that could serve as a groundwork to better grasp its pathophysiology and to estimate the amount of residual brain plasticity.

To address this gap, in this study we chose to explore the dynamics of brain activity during rs-fMRI in patients with progressive MS. In particular, we assessed: i) the potential of such neuroimaging

correlates to characterize this neurodegenerative stage of the disease, ii) whether the dynamics of brain functional patterns changed after one year of follow-up (FU), and iii) their role in explaining clinical disability.

Materials and Methods

Participants

Forty-eight patients with either PP or SP MS and 26 healthy controls (HC) were prospectively recruited. Diagnosis of PP or SP MS was made according to the revised McDonald's criteria 2010 (Polman *et al.*, 2011). Inclusion criteria were the following: i) age between 25 and 65 years, ii) expanded disability status scale (EDSS) score below 6.5 at screening, iii) if treated, patients had to be on a stable treatment for the previous year, iv) no history of relapses in the previous year. Exclusion criteria included: current or past history of major hematological, renal, hepatic, psychiatric or neurological disease (other than MS for the patient group) and contraindications to MRI. From the initial sample of 74 subjects, 4 patients were excluded because of failure in MRI processing (i.e. functional-structural co-registration) and 13 (1 healthy control, 12 patients) were excluded after motion scrubbing because more than 25% of volumes in their scans had a framewise displacement above the threshold of 0.5 mm (Power *et al.*, 2012; Parkes *et al.*, 2018), resulting in a final sample of 57 subjects (25 HC, 18 patients with PP MS and 14 patients with SP MS). All subjects underwent MRI and, on the same day, patients with PMS underwent clinical and neuropsychological evaluation, at the baseline. Thirty-five (16 HC and 19 patients, 11 with PP MS and 9 with SP MS) out of the 57 subjects included at baseline underwent MRI after 1-year of FU ([mean ±SD]= 11±2 months).

The study was approved by the Institutional Review Board of the Icahn School of Medicine at Mount Sinai, and all the subjects gave written informed consent to participate.

Clinical and neuropsychological assessment

Patients with PMS underwent neurological examination at baseline and FU including EDSS, timed 25-foot walking (T25FW) test, 9-hole peg test (9HPT), and neuropsychological assessment including symbol digit modalities test (SDMT), California verbal learning test second edition (CVLT-II) and the brief visuospatial memory test revised (BVMT-R). For the CVLT-II and the BVMT-R the first five or three recall trials were considered, respectively (Langdon *et al.*, 2012). Raw scores were transformed into T-scores according to (Parmenter *et al.*, 2010).

MRI acquisition

All the participants underwent MRI on a 3.0 T scanner (Magnetom Skyra, Erlangen, Siemens, Germany) using a 32-channel head coil and with a protocol including the following sequences: a) T2-weighted sequence: voxel size 0.5x0.5x3 mm, repetition time (TR) 8000 ms, echo time (TE) 95ms; b) 3D T1-weighted sequence: voxel size:0.8x0.8x0.8 mm, TR 3000 ms, TE 2.47 ms, flip angle 7°, inversion time 1000 ms); c) single shot gradient echo planar imaging (EPI) sequence for the resting state: voxel size: 2.1x2.1x2.1 mm, TR 1000 ms, TE 35 ms, multi-band acceleration factor 7, flip angle 60°, 400 volumes. During resting state fMRI subjects were asked to rest with their eyes closed.

Structural MRI analysis

T2 lesions were segmented and lesion volume obtained using a semiautomatic segmentation technique (Jim 7, Xinapse Systems, Northants, UK).

Functional resting state MRI preprocessing

Resting state fMRI data were preprocessed using SPM12 (FIL, UCL, UK). Complementary functions of the Data Processing Assistant for Resting-State fMRI (Chao-Gan and Yu-Feng, 2010) and the Individual Brain Atlases using Statistical Parametric Mapping toolboxes (Aleman-Gomez *et al.*, 2006) were also used. Preprocessing steps included: realignment and discarding of the first 10

volumes, resulting in 390 time-points. Then, the T1-weighted and functional images were co-registered, and the structural images were segmented into white matter (WM), grey matter and cerebrospinal fluid (CSF). Regression of the nuisance variables, including the average WM and CSF signals and the six motion parameters, was then performed using DPARSF toolbox. A spatial smoothing (Gaussian kernel of a 6 mm full width at half maximum) was finally applied.

Motion

We identified subjects that displayed too much motion characterized by their framewise displacement values (Power *et al.*, 2012). Those with FD_{Power} >0.5 mm in more than 25% of the volumes (Parkes *et al.*, 2018) were excluded from the analysis. In the final sample, the average FD did not differ between patients with PMS and HC at the baseline ($t(55)= -1.37$, $p=0.18$) and at FU ($t(33)= -1.52$, $p=0.14$, see Table 1). In all other subjects, scrubbing was applied with contaminated volumes (FD_{Power}>0.5mm) censored and replaced by the spline interpolation of the previous and following volumes. Motion frames were excluded from the computation of iCAPs temporal properties.

iCAPs analysis

The analysis was performed using a publicly available implementation (https://c4science.ch/source/iCAPs/). In brief, a hemodynamic deconvolution was first applied using total activation (TA) to the single subject's native space fMRI time-courses at baseline and FU. The TA method uses prior information about the hemodynamic response function to deconvolve the fMRI time-series through a spatio-temporal regularization (Karahanoğlu *et al.*, 2013; Farouj *et al.*, 2017). Thereafter, fMRI frames corresponding to transients, obtained by the temporal derivative of the deconvolved time-series, were identified. These frames were normalized to the MNI coordinate space and were concatenated across all subjects. The resulting matrix "number of voxels x transients" underwent temporal k-means clustering to obtain brain patterns that

are simultaneously transitioning, i.e. iCAPs. Consensus clustering, a resampling based procedure for optimal class discovery (Monti *et al.*, 2003), was then used to determine the optimum number of clusters. As a last step, activity inducing time-courses for each subject were obtained for all iCAPs using spatio-temporal transient-informed regression (Zöller *et al.*, 2019). For further details about the TA procedure and the choice of the consensus clustering parameters, see the Supplementary Information (SI), Figure SI 1 and Figure SI 2.

iCAPs temporal properties

To retrieve the temporal properties, the time-courses were Z-scored within each subject and thresholded at $|z| > 1$ to determine the "active" time-points. We then derived: i) the total duration of overall activation as the percentage of the total non-motion scanning time for each iCAPs, ii) the *coupling*s and iii) *anti-coupling*s, which pertain to the number of time-points between pairs of iCAPs with similar signed co-(de)activation) and opposite signed co-(de)activation, respectively. This is equivalent to the Jaccard index, i.e. the number of time-points during which the two iCAPs were both active divided by the number of time-points during which at least one of them was active (Figure SI 3).

Analysis at follow-up

The TA analysis was applied to the 35 subjects at follow-up (FU). Then, the iCAPs retrieved from the baseline sample were fitted into the FU sample. This was done by matching each significant innovation frame of subjects at FU to the closest iCAP obtained from baseline using cosine distance, as a metric. After obtaining the cluster index for the innovation frames at FU and their distance to each cluster center, the transient-informed regression step was repeated on FU data to obtain each subject's iCAP time-courses and their corresponding temporal properties.

Statistical analysis

Demographic and clinical parameters were compared using unpaired and paired t-test between HC and patients with PMS or between values at baseline and FU, respectively.

ANCOVA was used to compare iCAPs duration between HC and PMS patients, using age, gender and education as covariates and a false discovery rate (FDR) correction according to (Benjamini *et al.*, 1995) was applied. To compare FU and baseline iCAPs temporal properties, a repeated measure ANCOVA analysis was used considering the PMS patients vs HC group x time interaction. Further analyses on coupling/anti-coupling features were computed only for iCAPs whose duration was significantly different between HC and PMS patients.

Partial least squares correlation (PLSC) analysis (Krishnan *et al.*, 2011) was used to investigate patterns of correlation between clinical parameters and temporal properties of iCAPs. Age, gender and education were step-wise regressed from each variable, except for the already normalized T scores of cognitive tests. According to the PLSC procedure, the [subjects x temporal properties] matrix X for brain variables (iCAPs temporal properties) and the [subjects x behavioral variables] matrix Y for clinical ones were built, concatenating HC and PMS patients. Their relationship was assessed by means of singular value decomposition of the correlation matrix between X and Y, which resulted in latent components that indicate multivariate patterns of brain-behavior correlation. The significance and stability of the components was assessed by permutation (1000 permutations) and bootstrap (800 bootstrap samples) testing, respectively. The toolbox used to run PLSC analysis is publicly available (https://miplab.epfl.ch/index.php/software/PLS).

We performed different combinations of PLSC analyses using the total iCAPs duration or coupling/anti-coupling with respect to the following behavioral scores in patients with PMS: i) the EDSS, ii) the upper and lower limb motor score tests; i.e., 9HPT and T25FW tests, and iii) the cognitive tests T scores (BVMT-R, CVLT-II and SDMT). Guided by the results of the correlation analyses with iCAPs duration (see Results section), we performed two complementary PLSC

analyses of the anti-couplings between $iCAP2_{Aud/SM}$ or $iCAP5_{AntDMN}$ and the other iCAPs and motor or cognitive test scores, respectively.

Data availability

Data supporting the findings of this study will be shared upon request.

Results

Demographic and clinical data

Demographic data for the two groups and clinical data for the patients with PMS are reported in Table 1. No significant differences were observed for age, gender and education between HC and PMS patients at the baseline and FU. Demographic and clinical data at baseline of the 35 subjects who underwent FU analysis are reported in the Table SI 1. PMS patients did not differ in terms of any clinical parameter of disability between baseline and FU.

Spatial properties of iCAPs

Baseline. Eleven iCAPs with different spatial distribution were obtained and considered for subsequent analysis. The large-scale networks represented in each iCAPs are shown in Figure 1 and named based on the observed spatial pattern and its overlap with well-known functional networks. These are the hippocampus/amygdala/basal ganglia ($iCAP1_{Hipp/Amy/BG}$), Auditory/Sensory-Motor ($iCAP2_{Aud/SM}$), primary visual ($iCAP3_{PrimVis}$), executive control network ($iCAP4_{ECN}$), anterior DMN ($iCAP5_{AntDMN}$), anterior Insula/Salience ($iCAP6_{AntIns/SAL}$), temporo-parietal/language ($iCAP7_{TempPar/LAN}$), secondary visual ($iCAP8_{SecVis}$), posterior DMN ($iCAP9_{PostDMN}$), amygdala/temporal pole ($iCAP10_{Amy/TempP}$) and orbitofrontal cortex ($iCAP11_{OFC}$). The overlap between the spatial pattern of each iCAPs and the Yeo 17 networks parcellation (Schaefer *et al.*,

2018) or the ICA-defined intrinsic connectivity networks by Shirer et al. (Shirer *et al.*, 2012) is reported in Table SI 2.

Temporal properties of iCAPs: inter-group differences

Healthy controls vs PMS patients at baseline. The overall durations of the iCAP5$_{AntDMN}$ and iCAP6$_{AntIns/SAL}$ were significantly reduced in patients with PMS compared to HC (F(1,52)=10.99, p=0.002 and F(1,52)=6.98, p=0.011, respectively), with the former surviving FDR correction (Figure 2A). This difference was further manifested in terms of the couplings of iCAP5$_{AntDMN}$ vs other iCAPs, showing specifically that the anti-coupling between iCAP5$_{AntDMN}$ and iCAP4$_{ECN}$ was significantly higher in HC compared to patients with PMS (F(1,52)=7.2, p=0.010, Figure 2B).

Healthy controls vs PMS patients at FU. No significant group x time interaction was found for the eleven iCAPs durations or for the couplings involving iCAP5$_{AntDMN}$. A group effect was confirmed for iCAP5$_{AntDMN}$ and iCAP6$_{AntIns/SAL}$ durations (F(1,30)=14.5, p=0.001 and F(1,30)=5.6, p=0.024, respectively) and the anti-coupling between iCAP5$_{AntDMN}$ and iCAP4 $_{ECN}$ (F(1,30)=12,0, p=0.002). Meanwhile, a group effect emerged for iCAP2$_{Aud/SM}$ (F(1,30)=13.3, p=0.001) and the anti-coupling between iCAP2$_{Aud/SM}$ and iCAP5$_{AntDMN}$ (F(1,30)=4.2, p=0.049). The bar plots representing the iCAPs' durations and couplings for iCAP5$_{AntDMN}$ at baseline and FU for HC and PMS patients are reported in Figure SI 4.

iCAPs temporal properties and clinical parameters at baseline

The three PLSC analyses disclosed significant latent components that revealed different patterns of iCAPs duration associated to the EDSS, motor or cognitive clinical scores (Figure 3, Figure SI 5). Specifically, the EDSS was associated to increased duration of iCAP1$_{Hipp/Amy/BG}$ and to decreased duration of the iCAP2$_{Aud/SM}$ and iCAP9$_{PostDMN}$ (p=0.048), (Figure 3A, Figure SI 5A). Both T25FW and 9HPT positively correlated to iCAP1$_{Hipp/Amy/BG}$ duration and inversely with iCAP2$_{Aud/SM}$, iCAP7$_{TempPar/LAN}$, and iCAP9$_{PostDMN}$ durations (p=0.032), (Figure 3B, Figure SI 5B). Cognitive

scores were associated to the $iCAP3_{PrimVis}$, $iCAP8_{SecVis}$, $iCAP5_{AntDMN}$ and $iCAP10_{Amy/TempP}$ durations (p=0.037). Specifically, the SDMT and BVMT-R were inversely associated to the $iCAP5_{AntDMN}$ and the SDMT positively with $iCAP3_{PrimVis}$ duration. Instead, CVLT-II was inversely associated to the duration of $iCAP8_{SecVis}$ and $iCAP10_{Amy/TempP}$ (Figure 3C, Figure SI 5C).

The PLSC analyses involving the anti-couplings between $iCAP2_{Aud/SM}$ and the other iCAPs and motor test scores, respectively, did not reach the significance (p=0.063, Figure SI 6).

A significant latent component for anti-couplings of $iCAP5_{AntDMN}$ and BVMT, CVLT and SDMT T scores was found (p=0.005, Figure 4, Figure SI 5D). In particular, the anti-coupling between $iCAP5_{AntDMN}$ $iCAP2_{Aud/SM}$ positively correlated with the CVLT and negatively with the SDMT. Moreover, CVLT positively correlated to the anti-coupling between $iCAP5_{AntDMN}$ and $iCAP6_{AntIns/SAL}$ but negatively to anti-coupling between $iCAP5_{AntDMN}$ and $iCAP10_{Amy/TempP}$.

Discussion

In this work we characterized, for the first time, the changes in the brain dynamic functional patterns occurring in PMS patients. In MS, modifications of the brain functional organization parallel the focal and diffuse structural damage. While the distribution and evolution of the latter have been better documented integrating multiple imaging techniques (Filippi *et al.*, 2019), the brain functional reorganization at rest in MS has been more difficult to frame and track through the subsequent stages of the disease. However, tackling the reshaping of functional patterns is of utmost importance especially in the progressive stages of the disease since few options are available to prevent further structural damage. Against this background, exploring the brain functional dynamic, or changes of resting state functional activity over time, compared to a static, or averaged, characterization, could provide a more comprehensive representation of the changes occurring after neural injury (Zalesky *et al.*, 2014; Lurie *et al.*, 2020).

The first contribution of this study was the application of a recent methodology introduced in the dynamic rs-fMRI field to a neurodegenerative disease. The iCAPs method allows to describe

resting-state fluctuations in terms of temporally-overlapping networks, and thus provide a more accurate network-level representation of brain function and between-network interactions. Specifically, our study showed that patients with PMS present changes in the temporal properties of functional networks, mainly involving the anterior DMN, compared to HC. This first finding, observed both at baseline and FU, reveals the key role of the anterior DMN functional dysfunction in progressive MS. The medial prefrontal cortex and the anterior cingulate cortex are involved in a large range of cognitive, emotional and motor processes (Gusnard *et al.*, 2001; Margulies *et al.*, 2007; De La Vega *et al.*, 2016; Wang *et al.*, 2020), and different studies have highlighted their functional heterogeneity. Among the regions whose activity decreases most during goal-oriented tasks in healthy adults (Gusnard and Raichle, 2001; Buckner *et al.*, 2008), the anterior DMN presents a reduced activity during rest with aging (Damoiseaux *et al.*, 2006) and an increased activation during cognitive tasks in aging (Sambataro *et al.*, 2010) and in patients with neurodegenerative disorders (Saykin *et al.*, 1999*a*), interpreted as a failure in deactivation or as a compensatory phenomenon. In patients with PMS, the anterior DMN showed reduced conventional functional activity and has been related to cognitive disability and to depression (Rocca *et al.*, 2010; Bonavita *et al.*, 2011). Our results revealed a reduced engagement of these regions in PMS patients along with an altered synchronization between anterior DMN and ECN and a decreased dynamic of the anterior insula/salience network. The triple-network model has been well documented in literature, with the salience network mediating the switch between the DMN and ECN (Sridharan *et al.*, 2008; Goulden *et al.*, 2014). Tentatively, we can hypothesize a dysfunction in the interaction among these three networks and an impaired functional dynamic among networks regulating the integration and balance between internally and externally oriented processes occurring in the progressive stage of MS. Such altered dynamics have a patent relationship with cognitive disability, as revealed by the negative and positive correlation with the $iCAP5_{AntDMN}$ duration and the anti-coupling between $iCAP5_{AntDMN}$ and $iCAP6_{AntIns/SAL}$, respectively. Within this framework, a potential interpretation of the lower functional dynamic of the anterior DMN as an attempt to adapt to

cognitive tasks demand. This hypothesis warrants further investigations in studies of the functional dynamic during both rest and task paradigms.

A second relevant finding of our study was the stability of the functional dynamic dysfunction over time in patients with PMS. The longitudinal variation of brain functional activity in patients with PMS has been poorly investigated and, to our knowledge, only a longitudinal study focusing on the sensory-motor network and the relationship between FC and brain gamma-aminobutyric acid levels, has been performed (Droby *et al.*, 2020). Although the data only covers a short time lapse (one year), our results did not show any significant change in dynamics of functional patterns in PMS patients, which paralleled a steadiness in clinical disability in the PMS patients' group. However, further longitudinal studies with longer follow-up or with a larger sample size will help in addressing whether more subtle brain functional modifications occur in MS patients in the progressive phase over a longer time frame.

Finally, we established several relationships between iCAPs' durations and combined scores of clinical disabilities. The global disability, as expressed by the EDSS, was related to the $iCAP1_{Hipp/Amy/BG}$, the $iCAP2_{Aud/SM}$ and the $iCAP9_{PostDMN}$ duration. The DMN and the sensory-motor networks are frequently reported to show altered rs-FC properties in patients with MS since the early stage of the disease and through the relapsing remitting phase (Roosendaal *et al.*, 2010; Rocca *et al.*, 2012). A direct relation between static FC and EDSS in PMS has not been previously reported, with the exception of a post-hoc analysis on a subsample of patients with SP MS, showing no correlations between the rs-FC of the premotor cortex and EDSS (Dogonowski *et al.*, 2013). Nonetheless, two large studies conducted on large and phenotypically mixed sample described an inverse relationship between EDSS and rs-FC in the sensory-motor network and DMN (Rocca *et al.*, 2018; Pinter *et al.*, 2019).

It is noteworthy that, in the current work, we observe that the correlation between dynamic brain functional patterns and motor tests scores (both T25FW and 9HPT) mirrors the relationship between dynamic brain functional patterns and EDSS, involving the same iCAPs, with the

exception of the $iCAP7_{TempPar/LAN}$. For intermediate to high scores, the EDSS mainly reflects the impairment in walking and upper limbs, bulbar or every-day life functioning, respectively (Uitdehaag, 2014). Thus, in our sample of patients with a median EDSS of 5.75, the relationship between functional dynamic and EDSS could be mainly driven by the motor test scores.

The positive correlation between $iCAP1_{Hipp/Amy/BG}$ and motor scores or EDSS could imply a maladaptive role for the basal ganglia and the thalamus dynamic functional activity in the motor and global disability in patients with PMS. Ambulation has been related to pallidum and caudate atrophy (Motl *et al.*, 2015), but functional studies on the subcortical structures have shown a direct relation between basal ganglia rs-FC and fatigue in MS patients (Finke *et al.*, 2015). Moreover, thalamic static FC has been shown to predict EDSS in patients with a clinically isolated syndrome (Hidalgo de la Cruz *et al.*, 2020). Another possible interpretation of this finding is the negative effect of an abnormal engagement in the temporal regions of $iCAP1_{Hipp/Amy/BG}$ would have on motor performance. In line with previous studies (Rocca *et al.*, 2018; Pinter *et al.*, 2019), the duration of $iCAP2_{Aud/SM}$ and $iCAP9_{PostDMN}$ inversely correlated with EDSS. However, our study, for the first time, revealed this association in a sample of progressive MS patients and found a correlation between other parameters of motor disability and the same networks. Lastly, although the temporo-parietal regions have not been associated to motor disability in patients with MS, they are associated to gait control (Takakusaki, 2017) and are involved in upper limbs tasks, attention and self-perception (Igelström and Graziano, 2017). To better interpret this result, it is noteworthy to point out that, although not statistically significant, the motor scores inversely correlated with the anti-couplings between $iCAP2_{Aud/SM}$ and either $iCAP7_{TempPar/LAN}$ or $iCAP9_{PostDMN}$. Further investigation would confirm whether the motor disability, in patients with PMS, is related to the dynamic interplay among the sensory-motor, temporo-parietal regions, and posterior DMN.

As per the relationship between FC and cognition, the DMN plays a pivotal role in the cognitive disability in patients with MS (Rocca *et al.*, 2010; Basile *et al.*, 2014). While a direct relationship between rs-FC and cognitive status was observed in patients at the progressive stages of the disease

(Rocca *et al.*, 2010), more studies have pointed out an inverse relationship, with an increased rs-FC of the DMN and salience network underlying the cognitive disability or the cognitive reserve (Hawellek *et al.*, 2011; Basile *et al.*, 2014; Bizzo *et al.*, 2020). Our results indicated that an increased engagement of the anterior DMN together with a reduced anti-coupling with areas of the salience network ($iCAP6_{AntIns/SAL}$) were associated to a worse cognitive performance in patients with PMS. However, we found a decreased duration of the $iCAP5_{AntDMN}$ in PMS patients compared to HC. In addition, data from literature suggests an influence for functional dynamic during rest on the subsequent performance during tasks (Gonzalez-Castillo and Bandettini, 2018), hence a possible interpretation of the reduced anterior DMN dynamic as compensatory. A reduced anti-coupling between $iCAP5_{AntDMN}$ and $iCAP2_{Aud/SM}$ correlated with a worse performance at CVLT-II but better for SDMT. While the former would indicate that the segregation between anterior DMN and auditory regions influences CVLT-II performance, the latter again suggests a compensatory role for the $iCAP5_{AntDMN}$, in this case involving its synchronicity with sensory-motor regions, probably the supplementary motor area functionally involved during SDMT (Silva *et al.*, 2018). We also confirmed an association between reduced dynamic of the visual network and cognitive impairment, previously observed in a study on a large sample of patients with relapsing-remitting, PP and SP MS (Eijlers *et al.*, 2019). Lastly, both the medial temporal and the prefrontal regions have been shown to activate during verbal processing (Saykin *et al.*, 1999*b*). Complementary, our results showed that the increased anti-coupling between $iCAP5_{AntDMN}$ and $iCAP10_{Amy/TempP}$ was associated with a worse performance at CVLT-II. Our findings highlight the complexity and diversity of the relationship between cognitive performance and functional brain patterns in PMS and suggest how a dynamic approach would better tackle it and disentangle its components.

This study has several limitations, including the small sample size at FU and the lack of motor and cognitive test scores on the HC group. The latter urges caution in the interpretation of the correlation analyses and future studies are needed to assess how the relationship between brain and behavioral data differ in patients with PMS, compared to HC. Moreover, further longitudinal

studies in the progressive stage, covering larger time intervals, are needed to better characterize the occurring functional reorganization.

In conclusion, functional brain dynamics in patients with progressive MS reveal significant changes at the level of the anterior DMN and disclose their potential role in better understanding the functional modifications underlying clinical disability. These alterations seem to closely reflect the clinical status, being both stable after a year follow-up.

Disclosures: Giulia Bommarito, Anjali Tarun, Younes Farouj, Maria Giulia Preti, Maria Petracca, Amgad Droby, Mohamed Mounir El Mendili, and Dimitri Van De Ville have nothing to disclose. Matilde Inglese is currently receiving a grant from Teva Neuroscience.

Funding: G. Bommarito was supported by a research fellowship FISM-Fondazione Italiana Sclerosi Multipla, Cod.: 2017/B/2 and financed or co-financed with the '5 per mille' public funding. A. Tarun and Y. Farouj were supported by the Swiss National Science Foundation under the Project Grant 205321-163376.

Figure 1.

Spatial patterns of the 11 iCAPs retrieved from the analysis on HC and patients with PMS. Under each iCAP the average consensus and the number of innovation frames assigned to it. Coordinates refer to the Montreal Neurological Institute space. Hipp: hippocampus; Amy: amygdala; BG: basal ganglia; ECN: executive control network; DMN: default mode network; LAN: language; TempPole: temporal pole; OFC: orbito-frontal cortex.

Figure 2.

A. Bar plots of the duration of the 11 iCAPs in the HC and patients with PMS patients. B. Anti-coupling between $iCAP4_{ECN}$ and $iCAP5_{AntDMN}$ resulted significantly different between the HC and PMS patients. Hipp: hippocampus; Amy: amygdala; BG: basal ganglia; Aud: auditory; SM: sensory-motor; ECN: executive control network; AntDMN: anterior default mode network; AntIns: anterior insula; SAL: salience; TempPar: temporo-parietal; LAN: language; SecVis: secondary visual; PostDMN: posterior default mode network; TempPole: temporal pole; OFC: orbito-frontal cortex. *p<0.05, ** surviving FDR correction.

Figure 3.

Partial least squares correlation analyses performed to assess the relationship between iCAPs durations and (A) EDSS (p=0.048), (B) Motor test scores (p=0.032) or (C) Cognitive test T scores (p=0.037). In yellow the robust weights after bootstrapping, the error bars represent bootstrap intervals. Hipp: hippocampus; Amy: amygdala; BG: basal ganglia; Aud: auditory; SM: sensory-motor; ECN: executive control network; AntDMN: anterior default mode network; AntIns: anterior insula; SAL: salience; TempPar: temporo-parietal; LAN: language; SecVis: secondary visual; PostDMN: posterior default mode network; TempPole: temporal pole; OFC: orbito-frontal cortex; EDSS: expanded disability status scale; T25FW: timed 25-foot walking test; 9HPT: 9-hole peg test; BVMT-R: brief visual memory test revised; CVLT-II: California verbal learning test (second edition); SDMT: symbol digit modalities test.

Figure 4.

PLSC analysis results between Cognitive tests T scores (BVMT-R, CVLT-II and SDMT) and the anti-couplings between $iCAP5_{AntDMN}$, and all the other iCAPs. In yellow the robust weights after bootstrapping, the error bars represent bootstrap intervals. Hipp: hippocampus; Amy: amygdala; BG: basal ganglia; Aud: auditory; SM: sensory-motor; ECN: executive control network; AntDMN:

anterior default mode network; AntIns: anterior insula; SAL: salience; TempPar: temporo-parietal; LAN: language; SecVis: secondary visual; PostDMN: posterior default mode network; Amy: amygdala; TempPole: temporal pole; OFC: orbito-frontal cortex; BVMT-R: brief visual memory test revised; CVLT-II: California verbal learning test (second edition); SDMT: symbol digit modalities test.

References

Aleman-Gomez Y, Melie-García L, Valdés-Hernandez P. IBASPM: toolbox for automatic parcellation of brain structures. In: 12th Annual Meeting of the Organization for Human Brain Mapping. 2006. p. 11–15

Basile B, Castelli M, Monteleone F, Nocentini U, Caltagirone C, Centonze D, et al. Functional connectivity changes within specific networks parallel the clinical evolution of multiple sclerosis. Mult Scler J 2014; 20: 1050–1057.

Benjamini Y, Hochberg Y, Benjamini, Yoav HY. Benjamini and Y FDR.pdf. J R Stat Soc Ser B 1995; 57: 289–300.

Bizzo BC, Arruda-Sanchez T, Tobyne SM, Bireley JD, Lev MH, Gasparetto EL, et al. Anterior Insular Resting-State Functional Connectivity is Related to Cognitive Reserve in Multiple Sclerosis. J Neuroimaging 2020: 1–5.

Bonavita S, Gallo A, Sacco R, Della Corte M, Bisecco A, Docimo R, et al. Distributed changes in default-mode resting-state connectivity in multiple sclerosis. Mult Scler J 2011; 17: 411–422.

Buckner RL, Andrews-Hanna JR, Schacter DL. The brain's default network: Anatomy, function, and relevance to disease. Ann N Y Acad Sci 2008; 1124: 1–38.

Chao-Gan Y, Yu-Feng Z. DPARSF: A MATLAB toolbox for 'pipeline' data analysis of resting-

state fMRI. Front Syst Neurosci 2010; 4: 1–7.

Confavreux C, Vukusic S. Natural history of multiple sclerosis: A unifying concept. Brain 2006; 129: 606–616.

Cordani C, Valsasina P, Preziosa P, Meani A, Filippi M, Rocca MA. Action observation training promotes motor improvement and modulates functional network dynamic connectivity in multiple sclerosis. Mult Scler J 2019: 1–8.

d'Ambrosio A, Valsasina P, Gallo A, De Stefano N, Pareto D, Barkhof F, et al. Reduced dynamics of functional connectivity and cognitive impairment in multiple sclerosis. Mult Scler 2019: 1352458519837707.

Damoiseaux JS, Rombouts SARB, Barkhof F, Scheltens P, Stam CJ, Smith SM, et al. Consistent resting-state networks across healthy subjects. Proc Natl Acad Sci U S A 2006; 103: 13848–13853.

Dogonowski AM, Siebner HR, Soelberg Sørensen P, Paulson OB, Dyrby TB, Blinkenberg M, et al. Resting-state connectivity of pre-motor cortex reflects disability in multiple sclerosis. Acta Neurol Scand 2013; 128: 328–335.

Droby A, Fleysher L, Petracca M, Podranski K, Xu J, Fabian M, et al. Lower cortical gamma-aminobutyric acid level contributes to connectivity in sensory-motor inter-connected regions in progressive MS. Mult Scler Relat Disord 2020; 43: 102183.

Eijlers AJC, Wink AM, Meijer KA, Douw L, Geurts JJG, Schoonheim MM. Reduced Network Dynamics on Functional MRI Signals Cognitive Impairment in Multiple Sclerosis. Radiology 2019; 292: 449–457.

Farouj Y, Karahanoglu FI, Van De Ville D. Regularized spatiotemporal deconvolution of fMRI data using gray-matter constrained total variation. Proc - Int Symp Biomed Imaging 2017: 472–475.

Filippi M, Preziosa P, Rocca MA. Brain mapping in multiple sclerosis: Lessons learned about the human brain. Neuroimage 2019; 190: 32–45.

Finke C, Schlichting J, Papazoglou S, Scheel M, Freing A, Soemmer C, et al. Altered basal ganglia functional connectivity in multiple sclerosis patients with fatigue. Mult Scler 2015; 21: 925–934.

van Geest Q, Douw L, van ‘t Klooster S, Leurs CE, Genova HM, Wylie GR, et al. Information processing speed in multiple sclerosis: Relevance of default mode network dynamics. NeuroImage Clin 2018; 19: 507–515.

Gonzalez-Castillo J, Bandettini PA. Task-based dynamic functional connectivity: Recent findings and open questions. Neuroimage 2018; 180: 526–533.

Goulden N, Khusnulina A, Davis NJ, Bracewell RM, Bokde AL, McNulty JP, et al. The salience network is responsible for switching between the default mode network and the central executive network: Replication from DCM. Neuroimage 2014; 99: 180–190.

Guerra-Carrillo B, MacKey AP, Bunge SA. Resting-state fMRI: A window into human brain plasticity. Neuroscientist 2014; 20: 522–533.

Gusnard DA, Akbudak E, Shulman GL, Raichle ME. Medial prefrontal cortex and self-referential mental activity: relation to a default mode of brain function. Proc Natl Acad Sci U S A 2001; 98: 4259–4264.

Gusnard DA, Raichle ME. Searching for a baseline: Functional imaging and the resting human brain. Nat Rev Neurosci 2001; 2: 685–694.

Hawellek DJ, Hipp JF, Lewis CM, Corbetta M, Engel AK. Increased functional connectivity indicates the severity of cognitive impairment in multiple sclerosis. Proc Natl Acad Sci U S A 2011; 108: 19066–19071.

Hidalgo de la Cruz M, Valsasina P, Mesaros S, Meani A, Ivanovic J, Martinovic V, et al. Clinical predictivity of thalamic sub-regional connectivity in clinically isolated syndrome: a 7-year study [Internet]. Mol Psychiatry 2020Available from: https://doi.org/10.1038/s41380-020-0726-4

Igelström KM, Graziano MSA. The inferior parietal lobule and temporoparietal junction: A network perspective. Neuropsychologia 2017; 105: 70–83.

Karahanoğlu FI, Caballero-Gaudes C, Lazeyras F, Van De Ville D. Total activation: fMRI deconvolution through spatio-temporal regularization. Neuroimage 2013; 73: 121–134.

Karahanoglu FI, Van De Ville D. Transient brain activity disentangles fMRI resting-state dynamics

in terms of spatially and temporally overlapping networks. Nat Commun 2015; 6: 7751.

Krishnan A, Williams LJ, McIntosh AR, Abdi H. Partial Least Squares (PLS) methods for neuroimaging: a tutorial and review. Neuroimage 2011; 56: 455–475.

De La Vega A, Chang LJ, Banich MT, Wager TD, Yarkoni T. Large-scale meta-analysis of human medial frontal cortex reveals tripartite functional organization. J Neurosci 2016; 36: 6553–6562.

Langdon DW, Amato MP, Boringa J, Brochet B, Foley F, Fredrikson S, et al. Recommendations for a brief international cognitive assessment for multiple sclerosis (BICAMS). Mult Scler J 2012; 18: 891–898.

Lassmann H. Pathogenic mechanisms associated with different clinical courses of multiple sclerosis. Front Immunol 2019; 10: 1–14.

Leonardi N, Richiardi J, Gschwind M, Simioni S, Annoni JM, Schluep M, et al. Principal components of functional connectivity: A new approach to study dynamic brain connectivity during rest. Neuroimage 2013; 83: 937–950.

Lin SJ, Vavasour I, Kosaka B, Li DKB, Traboulsee A, MacKay A, et al. Education, and the balance between dynamic and stationary functional connectivity jointly support executive functions in relapsing–remitting multiple sclerosis. Hum Brain Mapp 2018; 39: 5039–5049.

Lurie DJ, Kessler D, Bassett DS, Betzel RF, Breakspear M, Kheilholz S, et al. Questions and controversies in the study of time-varying functional connectivity in resting fMRI. Netw Neurosci 2020; 4: 30–69.

Lv H, Wang Z, Tong E, Williams LM, Zaharchuk G, Zeineh M, et al. Resting-state functional MRI: Everything that nonexperts have always wanted to know. Am J Neuroradiol 2018; 39: 1390–1399.

Margulies DS, Kelly AMC, Uddin LQ, Biswal BB, Castellanos FX, Milham MP. Mapping the functional connectivity of anterior cingulate cortex. Neuroimage 2007; 37: 579–588.

Monti S, Tamayo P, Mesirov J, Golub T. Consensus clustering: A resampling-based method for class discovery and visualization of gene expression microarray data. Mach Learn 2003; 52: 91–118.

Motl RW, Hubbard EA, Sreekumar N, Wetter NC, Sutton BP, Pilutti LA, et al. Pallidal and caudate volumes correlate with walking function in multiple sclerosis. J Neurol Sci 2015; 354: 33–36.

Parkes L, Fulcher B, Yucel M, Fornito A. An evaluation of the efficacy, reliability, and sensitivity of motion correction strategies for resting-state functional MRI. Neuroimage 2018; 171: 415–436.

Parmenter BA, Testa SM, Schretlen DJ, Weinstock-Guttman B, Benedict RHB. The utility of regression-based norms in interpreting the minimal assessment of cognitive function in multiple sclerosis (MACFIMS). J Int Neuropsychol Soc 2010; 16: 6–16.

Petracca M, Saiote C, Bender HA, Arias F, Farrell C, Magioncalda P, et al. Synchronization and variability imbalance underlie cognitive impairment in primary-progressive multiple sclerosis. Nat Publ Gr 2017: 1–12.

Pinter D, Beckmann CF, Fazekas F, Khalil M, Pichler A, Gattringer T, et al. Morphological MRI phenotypes of multiple sclerosis differ in resting-state brain function. Sci Rep 2019; 9: 1–7.

Polman CH, Reingold SC, Banwell B, Clanet M, Cohen JA, Filippi M, et al. Diagnostic Criteria for Multiple Sclerosis : 2010 Revisions to the McDonald Criteria. 2011

Power JD, Barnes KA, Snyder AZ, Schlaggar BL, Petersen SE. Spurious but systematic correlations in functional connectivity MRI networks arise from subject motion. Neuroimage 2012; 59: 2142–2154.

Preti MG, Bolton TA, Van De Ville D. The dynamic functional connectome: State-of-the-art and perspectives. Neuroimage 2017; 160: 41–54.

Rocca MA, Hidalgo de La Cruz M, Valsasina P, Mesaros S, Martinovic V, Ivanovic J, et al. Two-year dynamic functional network connectivity in clinically isolated syndrome. Mult Scler J 2019: 1–14.

Rocca MA, Valsasina P, Absinta M, Riccitelli G, Rodegher ME, Misci P, et al. Default-mode network dysfunction and cognitive impairment in progressive MS. Neurology 2010; 74: 1252–1259.

Rocca MA, Valsasina P, Leavitt VM, Rodegher M, Radaelli M, Riccitelli GC, et al. Functional

network connectivity abnormalities in multiple sclerosis: Correlations with disability and cognitive impairment. Mult Scler J 2018; 24: 459–471.

Rocca MA, Valsasina P, Martinelli V, Misci P, Falini A, Comi G, et al. Large-scale neuronal network dysfunction in relapsing-remitting multiple sclerosis. Neurology 2012; 79: 1449–1457.

Roosendaal SD, Schoonheim MM, Hulst HE, Sanz-Arigita EJ, Smith SM, Geurts JJG, et al. Resting state networks change in clinically isolated syndrome. Brain 2010; 133: 1612–1621.

Sambataro F, Murty VP, Callicott JH, Tan H-Y, Das S, Weinberger DR, et al. Age-related alterations in default mode network: impact on working memory performance. Neurobiol Aging 2010; 31: 839—852.

Saykin AJ, Flashman LA, Frutiger SA, Johnson SC, Mamourian AC, Moritz CH, et al. Neuroanatomic substrates of semantic memory impairment in Alzheimer's disease: patterns of functional MRI activation. J Int Neuropsychol Soc 1999; 5: 377–392.

Saykin AJ, Johnson SC, Flashman LA, McAllister TW, Sparling M, Darcey TM, et al. Functional differentiation of medial temporal and frontal regions involved in processing novel and familiar words: An fMRI study. Brain 1999; 122: 1963–1971.

Schaefer A, Kong R, Gordon EM, Laumann TO, Zuo X-N, Holmes AJ, et al. Local-Global Parcellation of the Human Cerebral Cortex from Intrinsic Functional Connectivity MRI. Cereb Cortex 2018; 28: 3095–3114.

Shirer WR, Ryali S, Rykhlevskaia E, Menon V, Greicius MD. Decoding subject-driven cognitive states with whole-brain connectivity patterns. Cereb Cortex 2012; 22: 158–165.

Silva PHR, Spedo CT, Barreira AA, Leoni RF. Symbol Digit Modalities Test adaptation for Magnetic Resonance Imaging environment: A systematic review and meta-analysis. Mult Scler Relat Disord 2018; 20: 136–143.

Sridharan D, Levitin DJ, Menon V. A critical role for the right fronto-insular cortex in switching between central-executive and default-mode networks. Proc Natl Acad Sci U S A 2008; 105: 12569–12574.

Takakusaki K. Functional Neuroanatomy for Posture and Gait Control. J Mov Disord 2017; 10: 1–17.

Tuleasca C, Bolton TAW, Régis J, Najdenovska E, Witjas T, Girard N, et al. Normalization of aberrant pretherapeutic dynamic functional connectivity of extrastriate visual system in patients who underwent thalamotomy with stereotactic radiosurgery for essential tremor: A resting-state functional MRI study. J Neurosurg 2020; 132: 1792–1801.

Uitdehaag BMJ. Clinical outcome measures in multiple sclerosis [Internet]. 1st ed. Elsevier B.V.; 2014Available from: http://dx.doi.org/10.1016/B978-0-444-52001-2.00016-9

Wang S, Tepfer LJ, Taren AA, Smith D V. Functional parcellation of the default mode network: a large-scale meta-analysis. Sci Rep 2020; 10: 16096.

Zalesky A, Fornito A, Cocchi L, Gollo LL, Breakspear M. Time-resolved resting-state brain networks. Proc Natl Acad Sci U S A 2014; 111: 10341–10346.

Zhuang X, Walsh RR, Sreenivasan K, Yang Z, Mishra V, Cordes D. Incorporating spatial constraint in co-activation pattern analysis to explore the dynamics of resting-state networks: An application to Parkinson's disease. Neuroimage 2018; 172: 64–84.

Zöller D, Sandini C, Karahanoğlu FI, Padula MC, Schaer M, Eliez S, et al. Large-Scale Brain Network Dynamics Provide a Measure of Psychosis and Anxiety in 22q11.2 Deletion Syndrome. Biol Psychiatry Cogn Neurosci Neuroimaging 2019; 4: 881–892.

Zoller DM, Bolton TAW, Karahanoglu FI, Eliez S, Schaer M, Van De Ville D. Robust recovery of temporal overlap between network activity using transient-informed spatio-temporal regression. IEEE Trans Med Imaging 2019; 38: 291–302.

Table 1. Demographic and clinical data at baseline and follow-up.

	Baseline (n=57)			**Follow-up (n= 35)**		
	HS (n=25)	MS patients (n=32)	p-value†	HS (n=16)	MS patients (n=19)	p-value‡
Age	47.3±8.7	50.8±9.9	0.17	48.9±7.2	52.7±9.4	0.20
Gender (females, males)	10; 15	20; 12	0.09	7; 9	13; 6	0.14
Education	17.2±3.5	16.6±2.4	0.46	17.7±3.9	16.8±2.2	0.43
Disease duration	-	15.4±12.0		-	15.2±12.3	-
EDSS (median; range)	-	5.75; 1.0-6.5		-	5; 2.5-6.5	-
SDMT raw score **SDMT T-score**	-	46.3±15.5 35.9±14.6		-	51.3±13.3 42.6±15.0	-
BVMT-R raw score **BVMT-R T-score**	-	16.6±2.4 31.0±12.6		-	19.8±8.9 41.6±16.1	-
CVLT-II raw score **CVLT-II T-score**	-	54.8±13.2 51.9±13.5		-	58.7±13.3 57.3±13.6	-
T25FW	-	8.8±4.4		-	12.1±15.8	-
9HPT	-	32.1±10.4		-	34.2±20.3	-
T2 LV	-	8.5±10.3		-	7.0±10.0	-
Motion (FD_{Power})	0.17±0.05	0.19±0.08	0.18	0.16±0.04	0.19±0.07	0.14

All variables are expressed as mean ± standard deviation if not otherwise specified.

† unpaired t-test between HS (n=25) and MS patients (n=32) at baseline.
‡ unpaired t-test between HS (n=16) and MS patients (n=19) at FU.

BS-Sub: subsample of 35 subjects at baseline; EDSS: expanded disability status scale; SDMT: symbol digit modalities test; BVMT-R: Brief Visuospatial Memory Test–Revised; CVLT-II: CVLT-II California Verbal Learning Test Second Edition; T25FW: timed 25-foot walk test; 9HPT: 9-hole peg test; T2 LV: lesion volume in T2-weighted sequence; FD: framewise displacement.

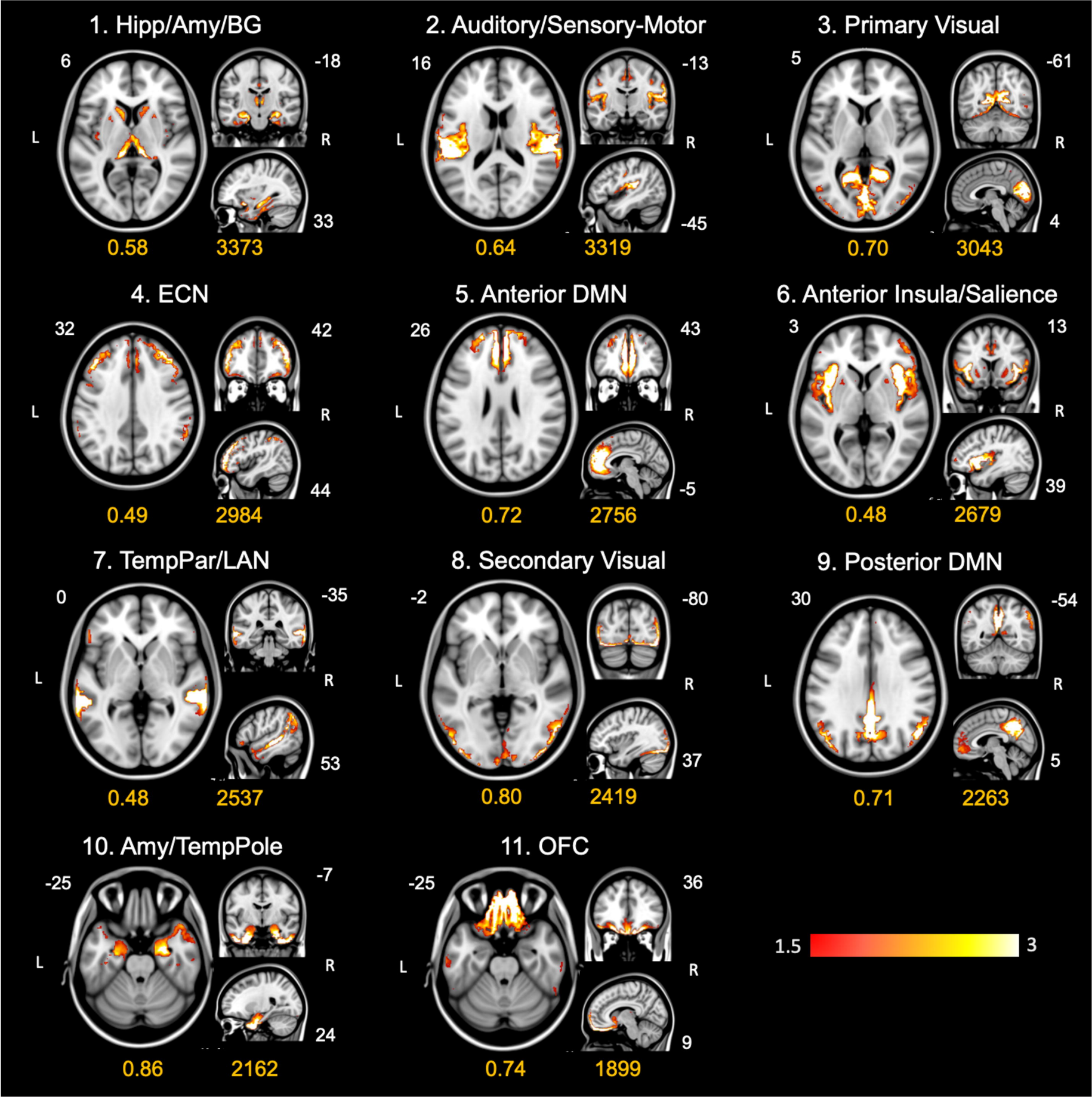
1. Hipp/Amy/BG
6
-18
L
R
33
0.58
3373
2. Auditory/Sensory-Motor
16
-13
L
R
-45
0.64
3319
3. Primary Visual
5
-61
L
R
4
0.70
3043
4. ECN
32
42
L
R
44
0.49
2984
5. Anterior DMN
26
43
L
R
-5
0.72
2756
6. Anterior Insula/Salience
3
13
L
R
39
0.48
2679
7. TempPar/LAN
0
-35
L
R
53
0.48
2537
8. Secondary Visual
-2
-80
L
R
37
0.80
2419
9. Posterior DMN
30
-54
L
R
5
0.71
2263
10. Amy/TempPole
-25
-7
L
R
24
0.86
2162
11. OFC
-25
36
L
R
9
0.74
1899
1.5
3

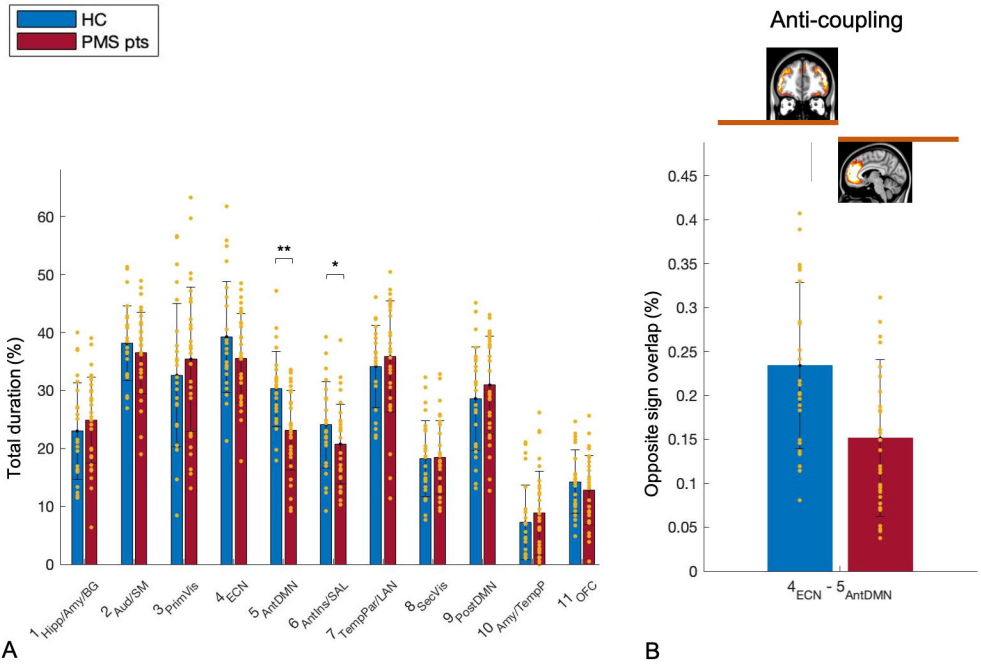
HC
PMS pts
Total duration (%)
0
10
20
30
40
50
60
**
*
1 Hipp/Amy/BG
2 Aud/SM
3 PrimVis
4 ECN
5 AntDMN
6 AntIns/SAL
7 TempPar/LAN
8 SecVis
9 PostDMN
10 Amy/TempP
11 OFC
A
Anti-coupling
Opposite sign overlap (%)
0
0.05
0.1
0.15
0.2
0.25
0.3
0.35
0.4
0.45
4 ECN - 5 AntDMN
B

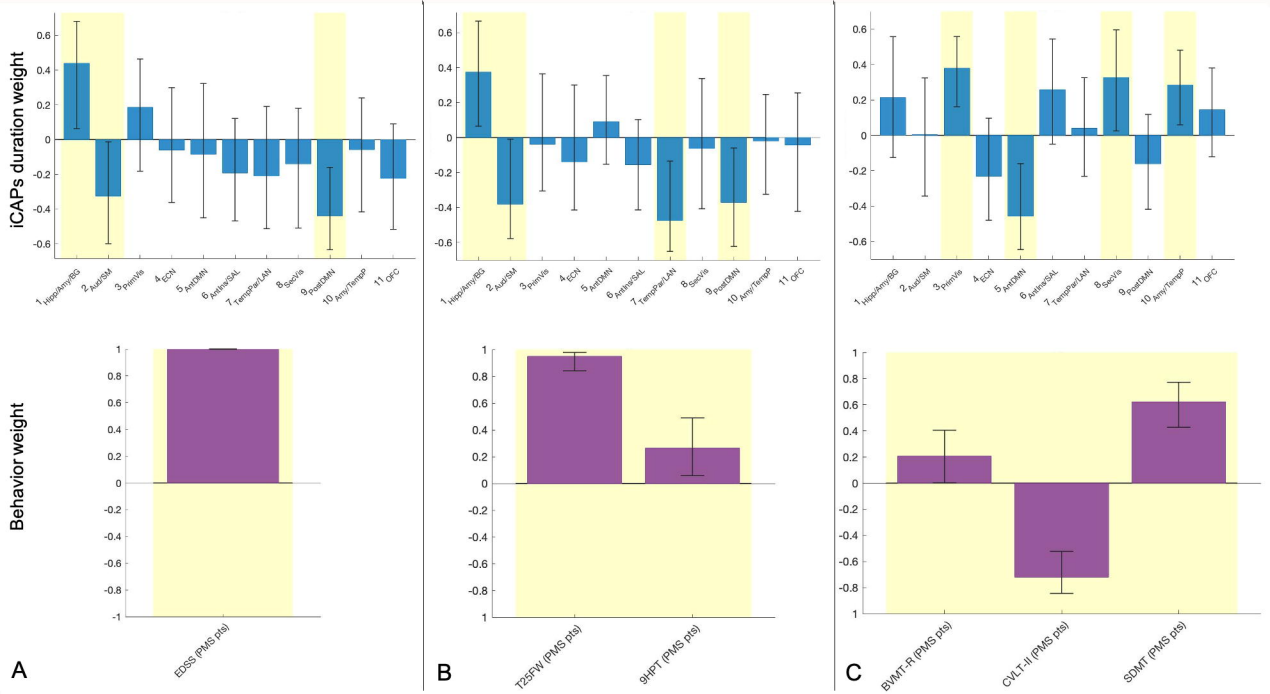
iCAPs duration weight
Behavior weight
1 Hipp/Amyg/BG
2 AudSM
3 PremVis
4 ECN
5 AntDMN
6 Antins/SAL
7 TempParLAN
8 SecVis
9 PostDMN
10 Amy/TempP
11 orC
EDSS (PMS pts)
T25FW (PMS pts)
9HPT (PMS pts)
BVMT-R (PMS pts)
CVLT-II (PMS pts)
SDMT (PMS pts)
A
B
C

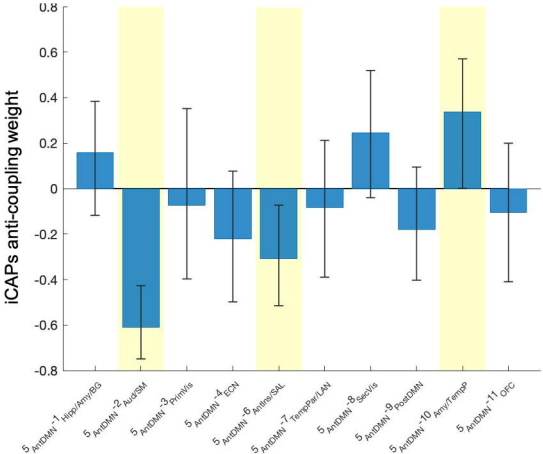
iCAPs anti-coupling weight
0.8
0.6
0.4
0.2
0
-0.2
-0.4
-0.6
-0.8
5 AntDMN-1 Hipp/Amy/BG
5 AntDMN-2 AudSM
5 AntDMN-3 PrimVis
5 AntDMN-4 CCN
5 AntDMN-6 AntIns/SAL
5 AntDMN-7 TempPar/LAN
5 AntDMN-8 SecVis
5 AntDMN-9 PostDMN
5 AntDMN-10 Amy/TempP
5 AntDMN-11 OFC

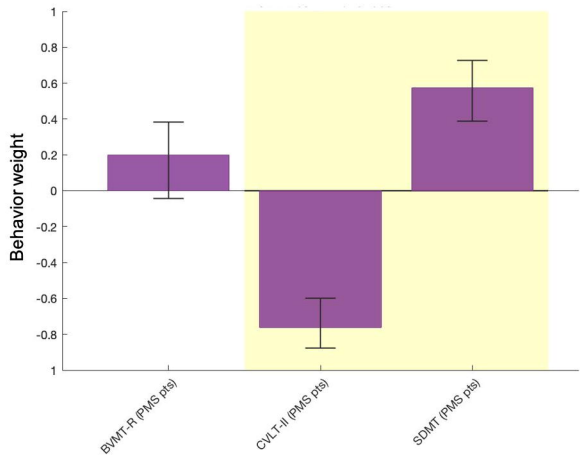
Behavior weight
1
0.8
0.6
0.4
0.2
0
-0.2
-0.4
-0.6
-0.8
1
BVMT-R (PMS pts)
CVLT-II (PMS pts)
SDMT (PMS pts)